

## Supporting information

# Pressure-induced structural phase transformation in cobalt(II) dicyanamide

**Andrey A. Yakovenko<sup>a</sup>, Karena W. Chapman<sup>a</sup> and Gregory J. Halder<sup>a\*</sup>**

<sup>a</sup>X-ray Science Division, Advanced Photon Source, Argonne National Laboratory, 9700 S Cass Ave, Argonne, Illinois, 60439, USA

Correspondence email: halder@aps.anl.gov

## S1. Synchrotron X-ray Powder Diffraction Analysis

### S1.1. *In situ* high pressure powder diffraction data

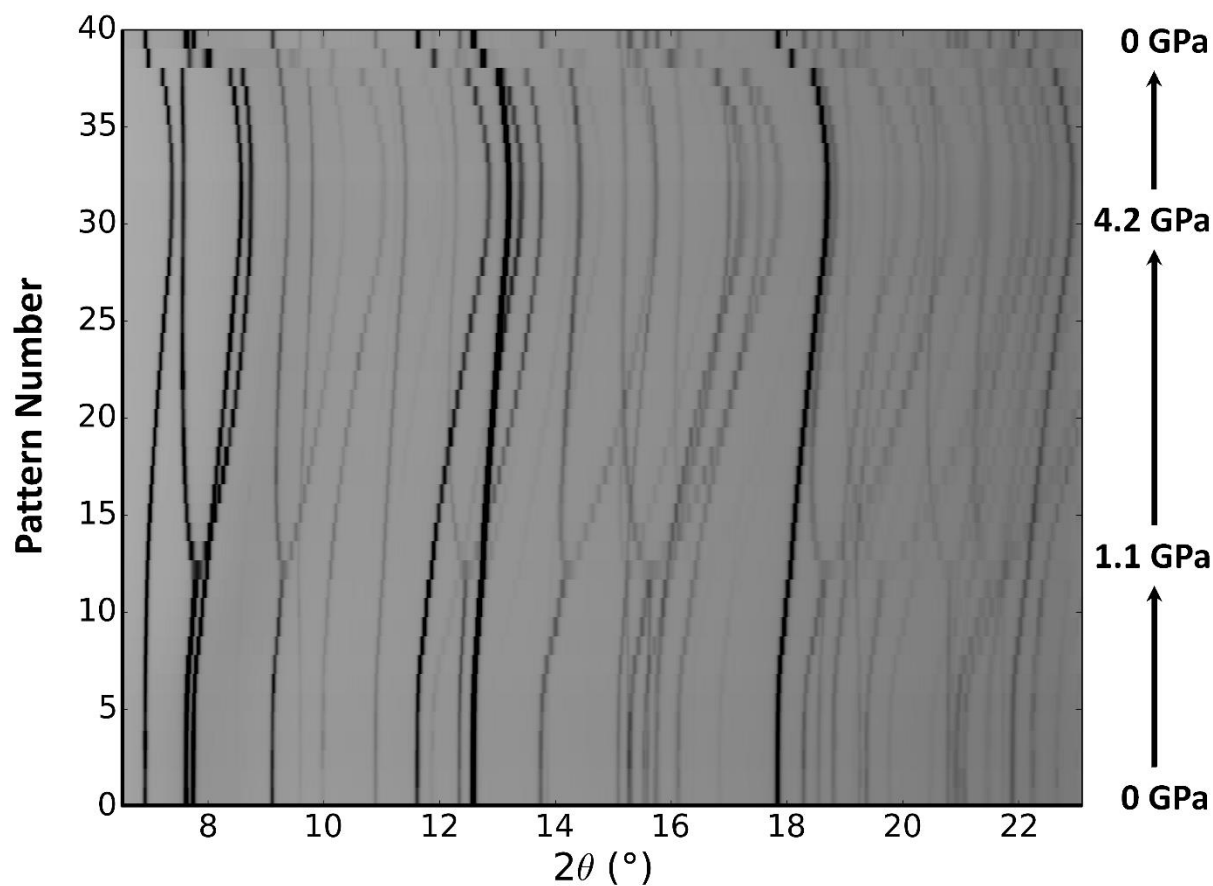


**Figure S1** Top view of the full range of powder diffraction patterns for  $\text{Co}[\text{N}(\text{CN})_2]_2$  from the *in situ* high-pressure experiment. Upon increase of the pressure, a transition from  $\alpha$  to  $\gamma$ -phase is observed at 1.1 GPa; no further phase transitions are observed up to the maximum measured pressure of 4.2 GPa. On gradual release of the pressure, the reverse transition back to the  $\alpha$ -phase is observed (also at  $\sim 1.1$  GPa).

## S1.2. Details for the Rietveld refinements

Collected and integrated *in situ* powder diffraction data sets were trimmed, normalized and plotted using *2DFLT* software. (Yakovenko, 2014) The Rietveld refinement was performed for the first pattern in the data set, using unit cell and structural parameters for the  $\alpha$ -Co[N(CN)<sub>2</sub>]<sub>2</sub> found previously (Kurmoo & J. Kepert, 1998). After satisfactory refinement parameters were reached, patterns with numbers from 1 to 11 (Fig. S1) were refined sequentially.

The high pressure phase,  $\gamma$ -Co[N(CN)<sub>2</sub>]<sub>2</sub>, was indexed using pattern number 32 (4.2 GPa) in the *GSAS-II* program (Toby & Von Dreele, 2013). It was found to be monoclinic with unit cell lengths similar to the  $\alpha$ -phase and a  $\beta$ -angle of  $\sim 98^\circ$ . After analysis of systematic absences in the pattern it was determined to have space group  $P 2_1/n$ , which was confirmed by performing LeBail whole pattern fitting.

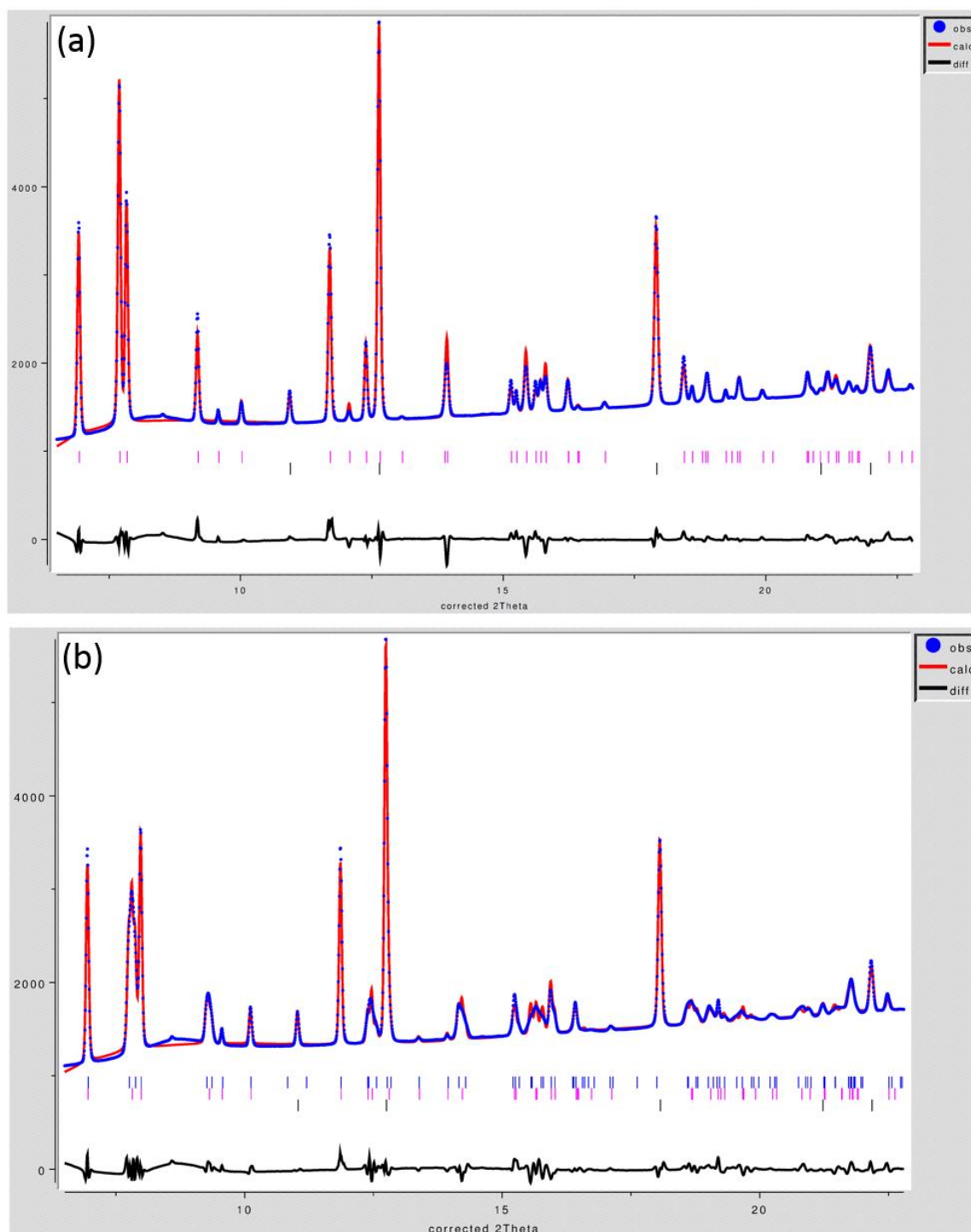
The initial structural parameters for the refinement of  $\gamma$ -Co[N(CN)<sub>2</sub>]<sub>2</sub> at 4.2 GPa were generated by using known atomic coordinates from  $\alpha$ -Co[N(CN)<sub>2</sub>]<sub>2</sub> with the addition of mirrored dicyanamide atoms. The occupancies of Co and amide N atom were doubled accordingly. The structure of the  $\gamma$ -Co[N(CN)<sub>2</sub>]<sub>2</sub> was gradually refined by applying the non-linear Marquardt technique using a fudge factor of 2 (Marquardt, 1963), allowing the atomic structure to adapt to the lower symmetry settings. The bond lengths and angles for the most rigid parts of the dicyanamide ligands were assumed to be minimally effected by pressure by applying the following restraints: C $\equiv$ N to  $\sim 1.15$  Å, C-N to  $\sim 1.32$  Å and N-C $\equiv$ N bond angles to  $\sim 180^\circ$ . The structures of  $\gamma$ -Co[N(CN)<sub>2</sub>]<sub>2</sub> at the lower pressure steps (31 to 14) were refined sequentially using parameters for the 4.2 GPa structure as the initial model in the refinement series.

The powder patterns at the transition pressure (numbers 12 and 13) contain diffraction peaks corresponding to both  $\alpha$ - and  $\gamma$ -Co[N(CN)<sub>2</sub>]<sub>2</sub>. Hence they were analysed using structural data from neighbouring patterns at (11 for  $\alpha$  and 14 for  $\gamma$ ) as initial models in the multiphase Rietveld refinements.

All Refinements also account for the presence of the NaCl pressure standard, which was refined using the well-established structural model.

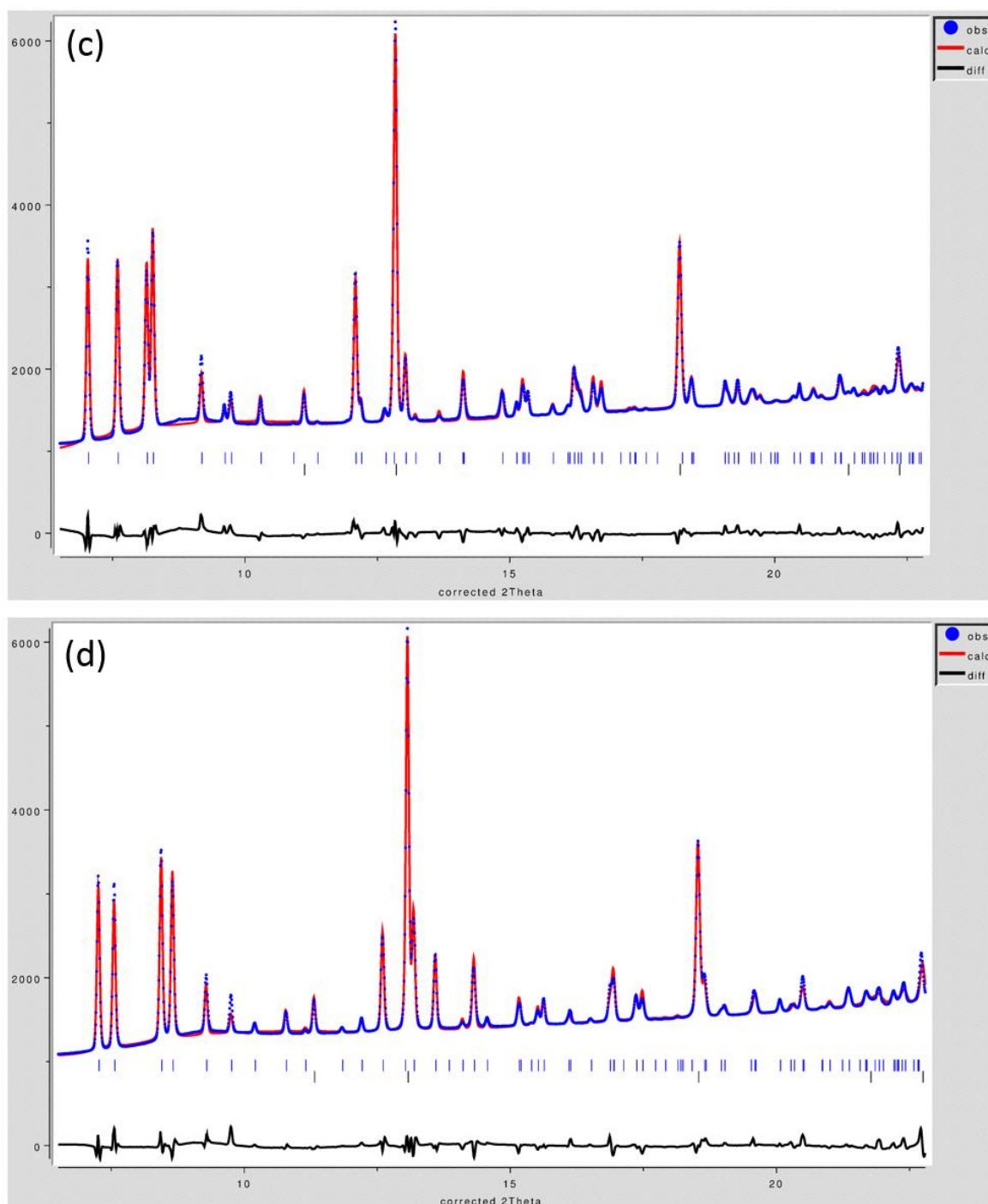
Crystal data and structure refinement parameters for selected patterns (numbers 8, 12, 17 and 26) are reported in Table S1. The final Rietveld plots for these patterns are reported on Figure S2. All data were refined using *Jana2006* (Petricek, 2006). Structures were visualized using the program packages *Diamond 4* (Putz & Brandenburg GbR, 2015) and *Crystal Maker* (Palmer *et al.*, 2014) while Rietveld plots were constructed using *pdCIFplot* (Toby, 2003).

Fig. S2, Part 1



(Part 2 of the Fig S2 located on the next page).

Fig. S2, Part 2



(Part 1 of the table located on the previous page)

**Figure S2** Final Rietveld refinement plots and difference profiles for the selected high-pressure data sets (a) number 8 – 0.37 GPa, (b) number 12 (two phase) – 1.03 GPa, (c) number 17 – 1.74 GPa, and number 26 – 3.60 GPa. For all plots Bragg peak tick-marks correspond to the following phases: magenta –  $\alpha$ -Co[N(CN)<sub>2</sub>]<sub>2</sub>, blue –  $\gamma$ -Co[N(CN)<sub>2</sub>]<sub>2</sub> and black – NaCl.

**Table S1** Refinement and crystal structure details from Rietveld fits for selected data sets.**Part 1**

Pattern [#]	<b>8</b>		<b>12</b>		
Pressure [GPa]	0.37		1.03		
$R_p, R_{wp}$	0.0128, 0.0207		0.0149, 0.0204		
GOF	0.83		0.82		
Phases	$\alpha$ -Co[N(CN) <sub>2</sub> ] <sub>2</sub>	NaCl	$\gamma$ -Co[N(CN) <sub>2</sub> ] <sub>2</sub>	$\alpha$ -Co[N(CN) <sub>2</sub> ] <sub>2</sub>	NaCl
Formula	C <sub>4</sub> N <sub>6</sub> Co	NaCl	C <sub>4</sub> N <sub>6</sub> Co	C <sub>4</sub> N <sub>6</sub> Co	NaCl
Phase mass %	66.05(7)	33.95(8)	38.0(2)	32.1(1)	29.92(7)
Crystal system	Orthorhombic	Cubic	Monoclinic	Orthorhombic	Cubic
Space group	<i>P mnn</i>	<i>F m-3m</i>	<i>P 2<sub>1</sub>/n</i>	<i>P mnn</i>	<i>F m-3m</i>
<i>a</i> [Å]	7.3967(2)	5.61290(4)	7.4088(3)	7.4177(3)	5.56722(4)
<i>b</i> [Å]	7.0737(1)	5.61290(4)	7.0087(2)	7.0071(2)	5.56722(4)
<i>c</i> [Å]	5.87615(8)	5.61290(4)	5.7309(2)	5.7274(2)	5.56722(4)
$\beta$ [deg]	90	90	90.892(3)	90	90
<i>V</i> [Å <sup>3</sup> ]	307.453(9)	176.832(2)	297.55(2)	297.70(2)	172.550(2)
<i>Z</i>	2	4	2	2	4
$D_{calc}$ [g·cm <sup>-3</sup> ]	2.0634	2.1952	2.132	2.131	2.250
$\mu$ [mm <sup>-1</sup> ]	1.834	1.199	1.878	1.901	1.214
$R_{Bragg}$	0.0654	0.0235	0.0605	0.0494	0.0116

**Part 2** of the table located on the next page

**Part 2**

Pattern [#]	<b>17</b>		<b>26</b>	
Pressure [GPa]	1.74		3.60	
$R_p, R_{wp}$	0.0154, 0.0213		0.0138, 0.0199	
GOF	0.85		0.79	
Phases	$\gamma$ -Co[N(CN) <sub>2</sub> ] <sub>2</sub>	NaCl	$\gamma$ -Co[N(CN) <sub>2</sub> ] <sub>2</sub>	NaCl
Formula	C <sub>4</sub> N <sub>6</sub> Co	NaCl	C <sub>4</sub> N <sub>6</sub> Co	NaCl
Phase mass %	65.30(7)	34.70(8)	63.47(7)	36.53(7)
Crystal system	Monoclinic	Cubic	Monoclinic	Cubic
Space group	$P 2_1/n$	$F m-3m$	$P 2_1/n$	$F m-3m$
$a$ [Å]	7.3976(2)	5.52405(4)	7.3377(2)	5.42870(3)
$b$ [Å]	6.8861(1)	5.52405(4)	6.5750(1)	5.42870(3)
$c$ [Å]	5.62799(9)	5.52405(4)	5.50296(8)	5.42870(3)
$\beta$ [deg]	94.9603(14)	90	98.0367(13)	90
$V$ [Å <sup>3</sup> ]	285.620(9)	168.567(2)	262.884(8)	159.988(2)
$Z$	2	4	2	4
$D_{calc}$ [g·cm <sup>-3</sup> ]	2.2211	2.3030	2.4132	2.4264
$\mu$ [mm <sup>-1</sup> ]	1.975	1.242	2.145	1.325
$R_{Bragg}$	0.0758	0.0190	0.0647	0.0167

**Part 1** of the table located on the previous page

## S2. Bulk Moduli and Linear Compressibility

Bulk moduli ( $B_0$ ) and linear compressibility ( $K$ ) values were calculated using the PASCAL program (Cliffe & Goodwin, 2012). Plots of these calculations are shown in Fig. S4 & Fig. S5.

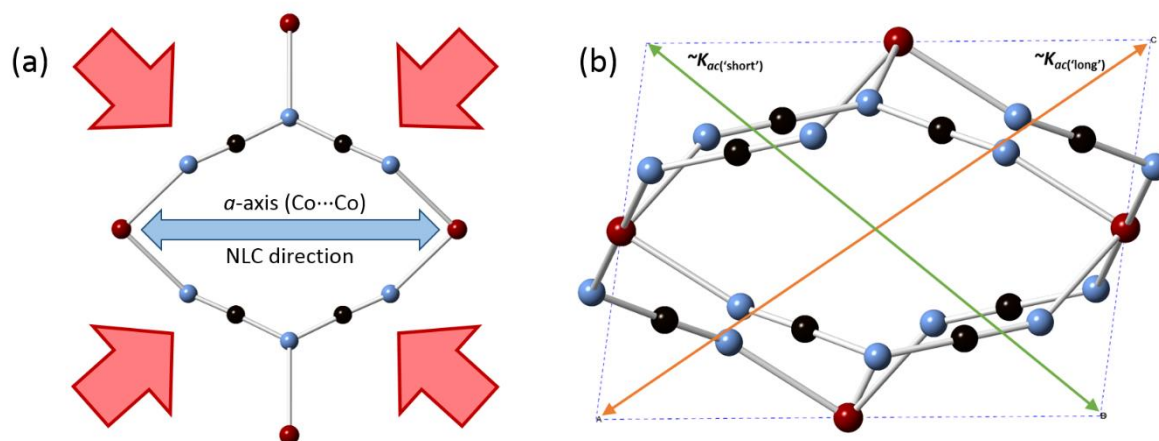


**Figure S3** (a) Schematic representation of the negative linear compressibility effect in  $\alpha$ -Co[N(CN)<sub>2</sub>]<sub>2</sub>. (b) Diagram showing “long” and “short” diagonals of  $ac$  plane in  $\gamma$ -Co[N(CN)<sub>2</sub>]<sub>2</sub>.



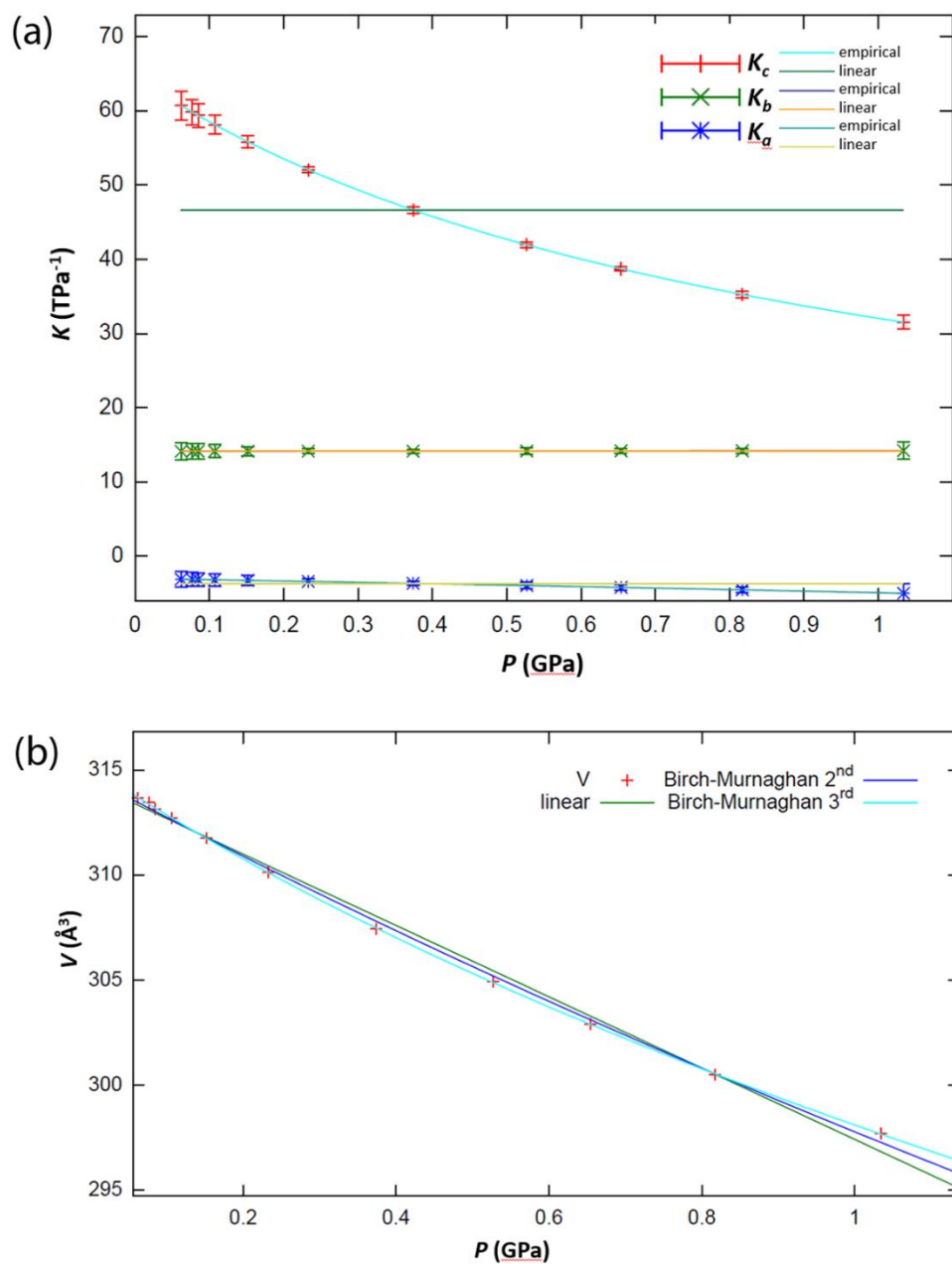


**Figure S4** (a) Calculations of the linear compressibility for  $\alpha\text{-Co}[\text{N}(\text{CN})_2]_2$ . (b) Fits of 2<sup>nd</sup> and 3<sup>rd</sup> order Birch–Murnaghan equations of state to the pressure-dependent lattice volume. The 3<sup>rd</sup> order model provides the best fit to the data to give  $B_0 = 13.15(18)$  GPa with a pressure-dependence of  $B' = 11.8(5)$ .

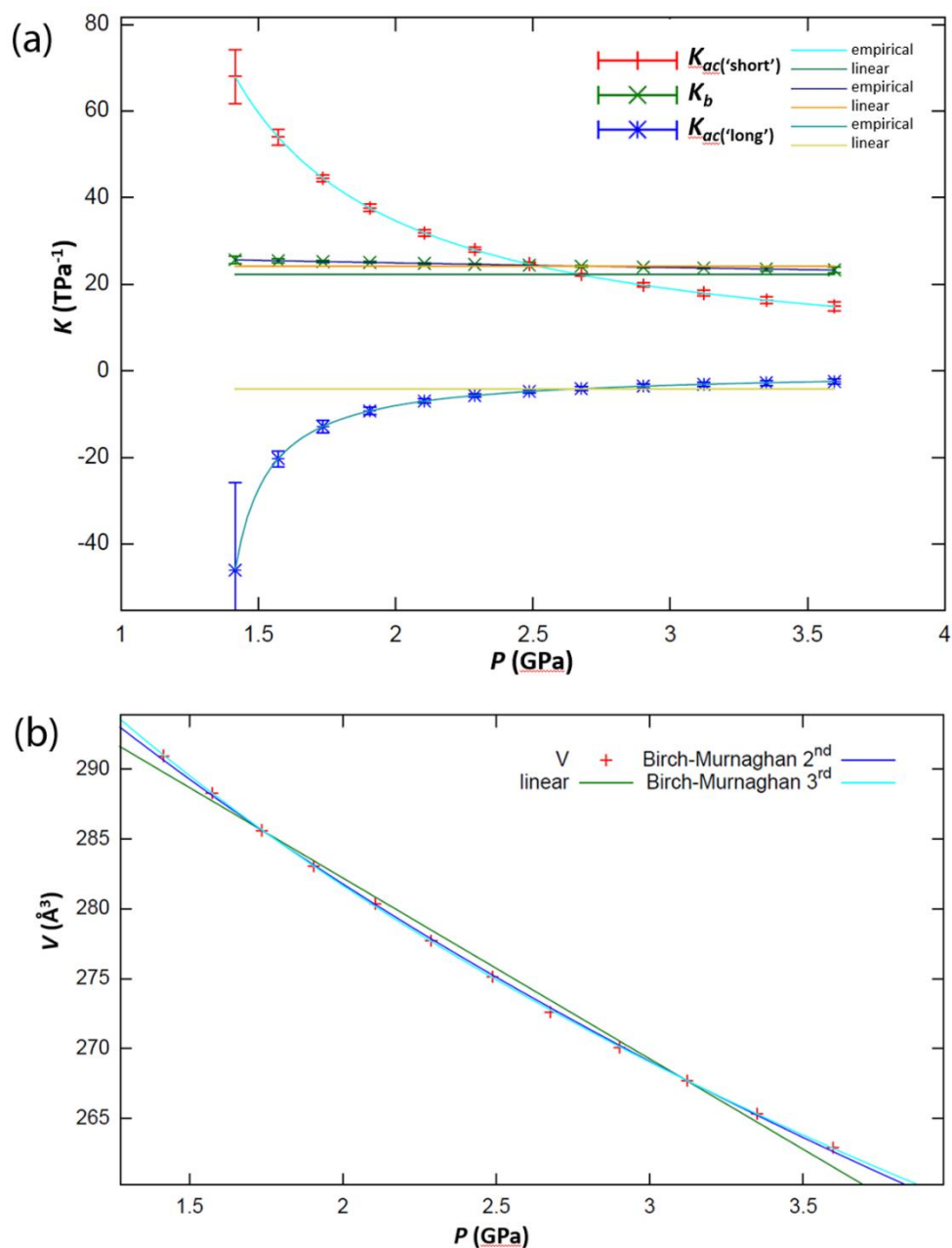


**Figure S5** (a) Calculations of the linear compressibility for  $\gamma\text{-Co}[\text{N}(\text{CN})_2]_2$  where  $K_{ac}(\text{'short'})$  and  $K_{ac}(\text{'short'})$  have direction matrices of  $(0.49, 0, 0.87)$  and  $(0.73, 0, -0.68)$ , respectively. (b) Fits of 2<sup>nd</sup> and 3<sup>rd</sup> order Birch–Murnaghan equations of state to the pressure-dependent lattice volume. The 3<sup>rd</sup> order model provides the best fit to the data to give  $B_0 = 9.0(6)$  with a pressure-dependence of  $B' = 11.8(5)$ .

## S3. Plots of selected structural parameters

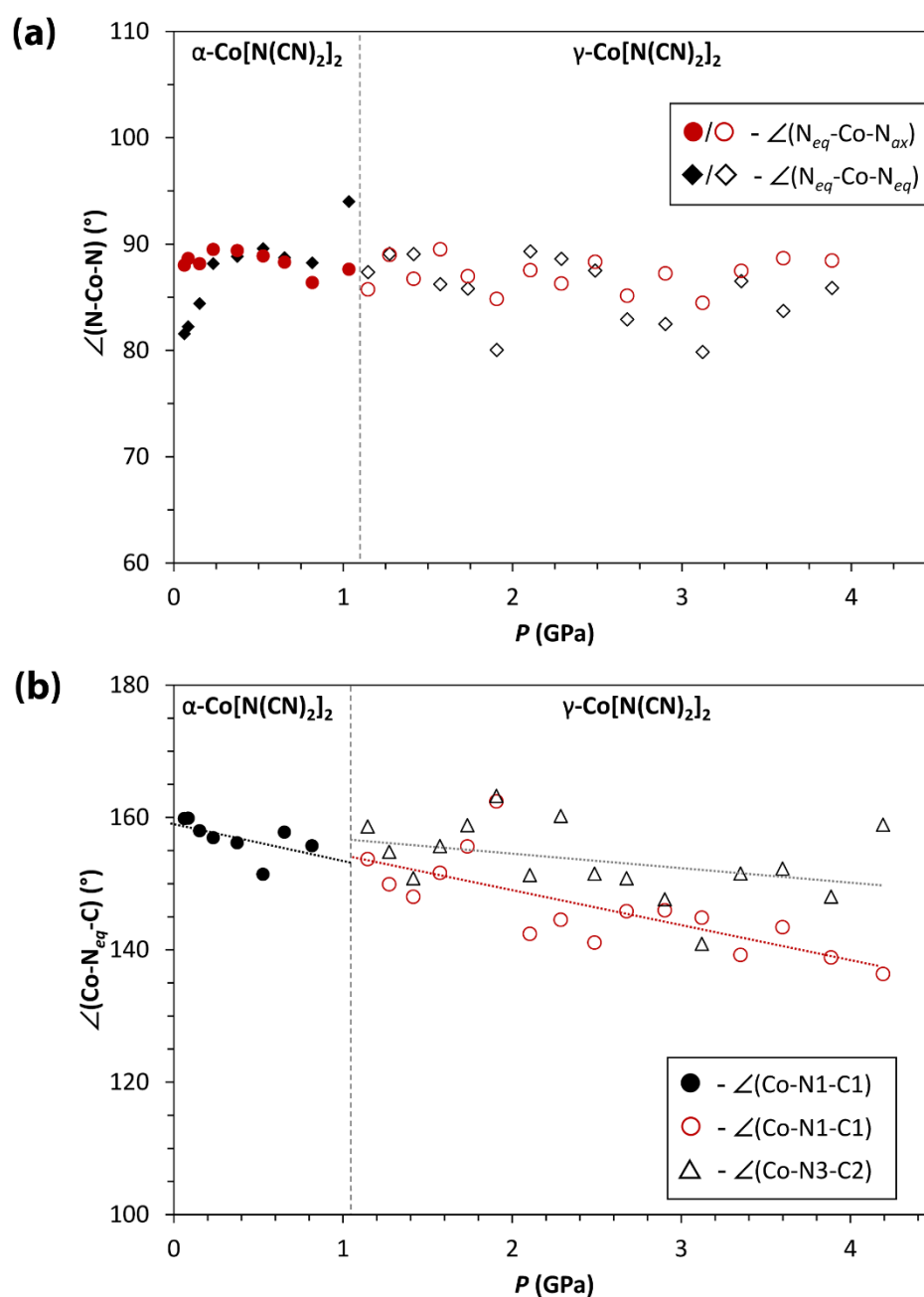


**Figure S6** Pressure-dependence of (a) the N-Co-N and (b) the amide Co-N<sub>eq</sub>-C bond angles for  $\alpha$ -Co[N(CN)<sub>2</sub>]<sub>2</sub> (solid markers) and  $\gamma$ -Co[N(CN)<sub>2</sub>]<sub>2</sub> (hollow markers). Vertical dashed lines indicate transition pressure where two phases are present. Other dashed lines represent linear fits to the data. No clear pressure-dependent trends were observed for the N-Co-N bond angles suggesting that the Co<sup>II</sup> octahedral remain relatively rigid. Errors are within the size of the data points.

**S4. References**

- Cliffe, M. J. & Goodwin, A. L. (2012). *J. Appl. Crystallogr.* 45, 1321-1329.
- Kurmoo, M. & J. Kepert, C. (1998). *New J. Chem.* 22, 1515-1524.
- Marquardt, D. W. (1963). *SIAM J. Appl. Math.* 11, 431-441.
- Palmer, D., Conley, M., Parsonson, L., Rimmer, L. & Stenson, I. (2014). *CrystalMaker ver. 9.1-Crystal Structures Visualization Software*. Oxfordshire, UK: CrystalMaker Software Ltd.
- Petricek, V., Dusek, M., Palatinus L. (2006). *Jana2006.Structure Determination Software Programs*. Praha, Czech Republic.: Institute of Physics.
- Putz, H. & Brandenburg, K. (2015). *Diamond 4 - Crystal and Molecular Structure Visualization*. Bonn, Germany: Crystal Impact.
- Toby, B. (2003). *J. Appl. Crystallogr.* 36, 1285-1287.
- Toby, B. H. & Von Dreele, R. B. (2013). *J. Appl. Crystallogr.* 46, 544-549.
- Yakovenko, A. A. (2014). *2DFLT ver.3.4.3. - Program for Normalization, Averaging and Editing of In Situ Data Sets*. Upton, NY, USA: Brookhaven National Laboratory.